

Dynamics of Two Overlapping Spin Ensembles Interacting by Spin Exchange

T.W. Kornack and M.V. Romalis

Department of Physics, Princeton University, Princeton, New Jersey 08544

(Received 6 August 2002; published 4 December 2002)

We describe linear and nonlinear dynamics of spin-polarized K and ^3He ensembles interacting by spin exchange. The interactions are dominated by the imaginary part of the spin-exchange cross section and each spin species is primarily affected by the average magnetization of the other. Operating in a very low magnetic field we demonstrate novel dynamics when the electron and nuclear spin precession frequencies are nearly matched. We observe transverse damping as well as a dynamic instability of the ^3He spins interacting with polarized K vapor. We also demonstrate operation as a self-compensating comagnetometer, useful for tests of *CPT* violation and other precision measurements.

DOI: 10.1103/PhysRevLett.89.253002

PACS numbers: 33.40.+f, 33.25.+k, 33.35.+r, 76.70.Dx

Spin exchange between alkali metals and noble gases has been extensively studied [1] and used in a wide range of applications, from searches for an electric dipole moment [2] and *CPT* violation [3] to imaging of human lungs [4]. The spin-exchange interaction of the form $\mathcal{H} = \alpha \mathbf{I} \cdot \mathbf{S}$ leads to both spin transitions and frequency shifts. For spin exchange between alkali metals and noble gases the frequency shifts are much larger than the transition rates. The frequency shifts of the alkali-metal spin resonance have been studied in [5–8], while the frequency shifts of the noble gas spin resonance have been investigated in [5,9]. In these experiments one of the spin species remained polarized along the magnetic field while the shift in the spin resonance of the other was measured.

In this Letter, we investigate spin-exchange effects between K vapor and ^3He gas in a very low magnetic field, such that the frequency shifts due to spin exchange are comparable to or larger than the Larmor frequencies. This leads to “hybrid” resonances where both spin species develop a transverse oscillating magnetization, somewhat akin to hybrid resonances in plasmas [10]. We investigate in detail the coupled K- ^3He oscillations following a small perturbation of the transverse magnetic field. We observe very large frequency shifts and strong damping of ^3He spin precession due to interaction with optically-pumped K vapor. For large perturbations from equilibrium the system behaves in a more complicated, nonlinear way. For example, if K and ^3He spins are polarized in opposite directions, we observe a dynamic instability leading to a spontaneous reversal of the ^3He polarization. Our measurements are well described by a set of coupled Bloch equations for K and ^3He atoms. Such equations, also known as the Bloch-Hasegawa equations [11], have been previously used to describe electron-spin resonance in metals doped with magnetic ions [12].

Our motivation for studying the K- ^3He system comes from the possibility of performing a test of *CPT* and Lorentz symmetry by looking for an anomalous magnet-iclike interaction [13]. Polarized K and ^3He can be used as a comagnetometer, allowing one to separate a *CPT*-

violating field from changes in the ordinary magnetic field [14]. We demonstrate self-compensating operation of the comagnetometer, where slow changes in the magnetic field are automatically canceled by interactions between the K and ^3He atoms, leaving only a signal proportional to the anomalous interaction that does not scale with the magnetic moments of the atoms. Comagnetometers involving two nuclear spins have been used for many precision measurements [2,3,15]. This is the first demonstration of a high-sensitivity comagnetometer involving a nuclear and an electron spin [16].

For most electron-electron spin-exchange processes the imaginary part of the spin-exchange cross section, which causes the frequency shift, is a small fraction of the real part. But for electron-nuclear spin exchange the imaginary part is 10^5 larger than the real part. The reason for this difference can be traced to the weakness of the spin-exchange interaction between alkali metals and noble gases, which induces only a small spin rotation angle ϕ during each collision. As a result, the spin transition probability proportional to ϕ^2 is much smaller than the frequency shift proportional to ϕ . We use the spin-exchange transitions to polarize ^3He nuclei over a period of several hours, but their effect on the dynamics discussed in this Letter can be safely ignored.

The frequency shifts due to spin exchange between a noble gas and an alkali metal can be represented by a magnetic field experienced by one species due to the magnetization of the other, $\mathbf{B} = \lambda \mathbf{M} = (8\pi\kappa_0/3)\mathbf{M}$ [5], where κ_0 is an enhancement factor over the classical magnetic field due to the attraction of the K electron wave function to the ^3He nucleus. For the K- ^3He system $\kappa_0 = 5.9$ at our operating temperature [8,17]. Including this interaction field leads to the following system of coupled Bloch equations for K electron and ^3He nuclear magnetizations \mathbf{M}^e and \mathbf{M}^n ,

$$\begin{aligned} \frac{\partial \mathbf{M}^e}{\partial t} &= \frac{\gamma_e}{S(\beta)} (\mathbf{B} + \lambda \mathbf{M}^n) \times \mathbf{M}^e + \frac{M_0^e \hat{z} - \mathbf{M}^e}{T_e S(\beta)}, \\ \frac{\partial \mathbf{M}^n}{\partial t} &= \gamma_n (\mathbf{B} + \lambda \mathbf{M}^e) \times \mathbf{M}^n + \frac{M_0^n \hat{z} - \mathbf{M}^n}{\{T_{2n}, T_{2n}, T_{1n}\}}. \end{aligned} \quad (1)$$

Here $\gamma_e = g\mu_B/\hbar = 2\pi \times 2.8 \text{ MHz/G}$ and $\gamma_n = \mu_{^3\text{He}}/\hbar = 2\pi \times 3244 \text{ Hz/G}$ are the electron and nuclear gyromagnetic ratios. For ^3He spins the longitudinal and transverse relaxation times are T_{1n} and T_{2n} , whereas for electron spins we use a common relaxation time T_e . $S(\beta)$ is the “slowing-down factor” due to sharing of the angular momentum between K electron and nuclear spins. In our regime of fast K-K spin exchange $S(\beta)$ depends on the electron spin temperature β and ranges from $S = 6$ for small electron polarization to $S = 4$ for polarization approaching unity [18]. M_0^e and M_0^n are the equilibrium magnetizations of K and ^3He , created by optical pumping for K and by spin-exchange transitions for ^3He .

The experiment is performed using a pump and probe laser arrangement shown in Fig. 1. A 2.5 cm diam spherical cell made from GE180 aluminosilicate glass contains at room temperature a small droplet of potassium metal, 3 atm of ^3He and 30 torr of N_2 to quench the excited state of K atoms. The cell is heated to 180°C by flowing hot air to obtain K vapor density of about $6 \times 10^{13} \text{ cm}^{-3}$. It is shielded by a set of five cylindrical magnetic shields with a shielding factor of 10^6 . A three-axis coil set provides control of the magnetic field inside the shields. K atoms are optically pumped along the \hat{z} axis using about 100 mW from a multi-mode diode laser tuned to the center of the K $D1$ line at 770 nm. The transverse polarization of K vapor in the \hat{x} direction is measured using optical rotation of a 50 mW single frequency linearly polarized probe beam detuned by about 1 nm to the blue of the $D1$ line.

In typical operating conditions the K electron spins experience a magnetic field generated by the ^3He magnetization of about $\lambda M_0^n = 1 \text{ mG}$. The ^3He spins experience a field generated by the electron magnetization of about $\lambda M_0^e = 20 \mu\text{G}$. The transverse and longitudinal relaxation times of ^3He are 1000 sec and 2 h, determined by

relaxation in magnetic field gradients [19]. The electron-spin relaxation time T_e is 5–10 msec, determined by the total pumping rate of the pump and probe lasers and spin-destruction collisions [18]. In both Eqs. (1) the magnetic interactions are larger than the dissipation terms. We make measurements with the magnetic field \mathbf{B} opposite to $\lambda\mathbf{M}^n$, such that $\mathbf{B} + \lambda\mathbf{M}^n$ is small compared with $\mathbf{B} + \lambda\mathbf{M}^e$. This allows us to match the resonance frequencies of electron and ^3He spins even though $\gamma_e \gg \gamma_n$.

The Bloch equations (1) include magnetic cross-coupling terms, but to a good approximation do not include self-interaction terms. ^3He atoms do not feel their own magnetization to first order because they are contained in a spherical cell. The asymmetry due to the “pull-off” of the glass cell is reduced by plugging the stem with a drop of K metal. Small deviations of the cell from a spherical shape lead to magnetic field gradients which reduce ^3He relaxation times T_{1n} and T_{2n} . The cross section for K-K spin exchange has a small imaginary component, about 10% of the real part [20]. However, the spin-exchange rate is much faster than all other rates and the expectation value of the electron spin is the same in both hyperfine states [18] so the electron spins do not feel any torque due to their own polarization.

For small transverse excitations of the spins the Bloch equations can be linearized, leading to the following solution for M_x^e that is directly measured in our setup:

$$\begin{aligned} M_x^e(t) &= \text{Re}[M_1 e^{-(A_e + A_n + F)t/2} + M_2 e^{-(A_e + A_n - F)t/2}], \\ A_n &= i\gamma_n(B_z + \lambda M_z^e) + T_{2n}^{-1}, \\ A_e &= [i\gamma_e(B_z + \lambda M_z^n) + T_e^{-1}]/S(\beta), \\ F &= [(A_n - A_e)^2 - 4\lambda^2\gamma_n\gamma_e M_z^e M_z^n / S(\beta)]^{1/2}, \end{aligned} \quad (2)$$

where M_1 and M_2 depend on the initial conditions. Thus, the response consists of two oscillations with different frequencies and decay rates. The coupling term F depends on the product of the two magnetizations, indicating the importance of mutual interactions between the spins.

Figure 2 shows the measured transient response of M_x^e following a small sudden step in the B_y field for several values of the external magnetic field B_z . Away from the resonance at $B_z \approx -\lambda M_z^n$, the transient responses clearly show the two decaying oscillations predicted by Eqs. (2). The faster oscillations correspond to the precession of the K electrons while the slow oscillations correspond to the precession of the ^3He nuclei. Close to the resonance at $B_z \approx -\lambda M_z^n$ the oscillations are no longer clearly distinguishable and are replaced by a hybrid response. The solid line in Fig. 2 is a fit based on Eqs. (2) using a common set of parameters for all transients. The fit parameters, such as equilibrium magnetizations and decay rates, are in good agreement with their independent determination using more direct measurements.

The frequencies and decay rates of the ^3He oscillations are summarized in Fig. 3. The solid line is a fit given by

$$2\pi\nu_n i + \Gamma_n = (A_e + A_n + F)/2. \quad (3)$$

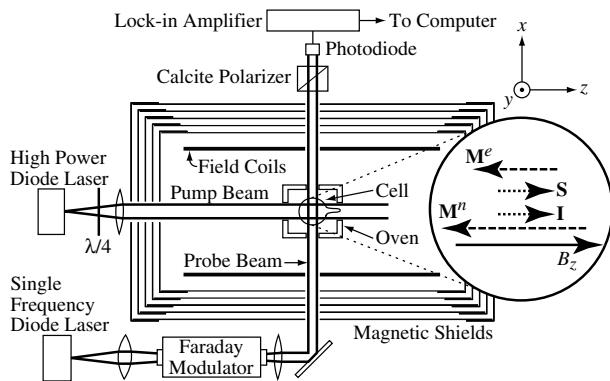


FIG. 1. Schematic of the apparatus used to investigate the coupled K- ^3He system. In the glass cell, the pump laser polarizes the K electron spins \mathbf{S} along the direction of the external magnetic field B_z , generating a K magnetization \mathbf{M}^e . The ^3He spins \mathbf{I} are polarized by spin-exchange transitions with K and generate a ^3He magnetization \mathbf{M}^n .

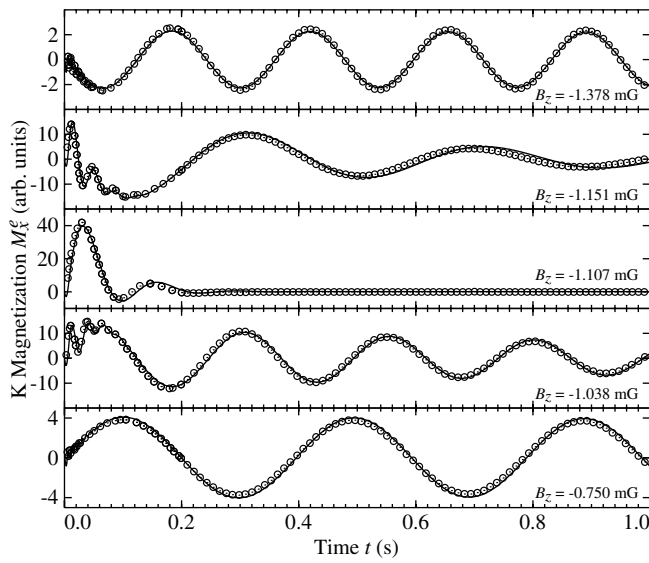


FIG. 2. The transient responses of the K electrons to transverse excitation of the coupled spin system as a function of the magnetic field B_z . The solid line is a common fit of the data based on Eq. (2).

The asymptotic behavior shown by the dashed lines corresponds to the frequencies of uncoupled K and ^3He oscillations. The changes in the frequencies are similar to an avoided level crossing.

For large excitations away from equilibrium the behavior of the spins is more complicated. Figure 4 shows the response following an RF pulse tipping ^3He magnetization such that $\gamma_e \lambda M_x^n T_e \gg 1$. In contrast to small excitations, the resulting signal is no longer a combination of exponential decays. The time for the signal to decay scales as a square of the initial tip angle ϕ . The ^3He

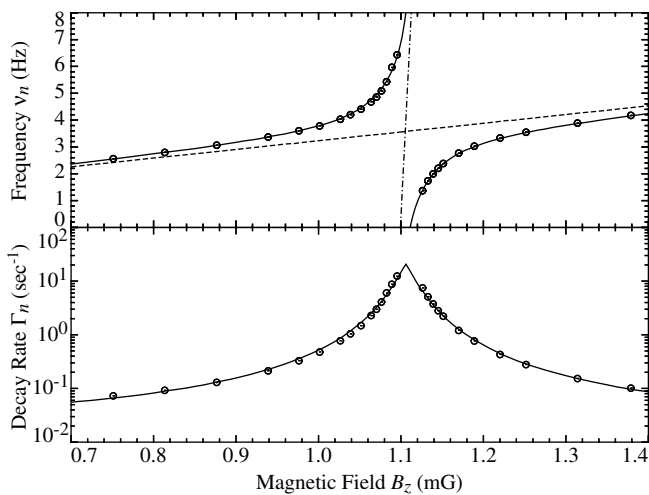


FIG. 3. The frequency and decay rate of the slowly decaying part of the transient response as a function the external field B_z . The solid line is a fit based on Eq. (3). Dashed lines show the Larmor frequencies of ^3He and K spins in the absence of interactions.

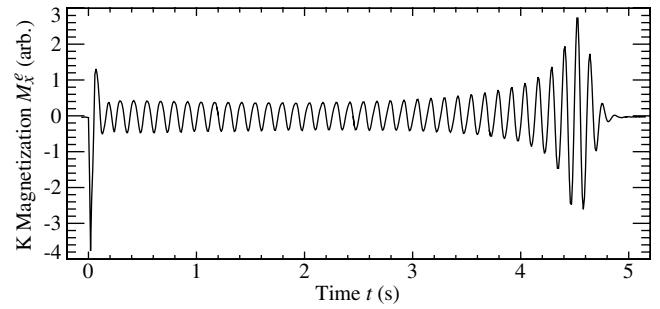


FIG. 4. Transient M_K^e signal following a $\phi = 14^\circ$ tip of the ^3He magnetization.

magnetization is rotated back along the \hat{z} axis by interactions with the K magnetic field, so that after the transient decays, M_z^n is larger than $M_0^n \cos(\phi)$. All of these features are well reproduced by numerical solutions of the coupled Bloch equations.

Even more dramatic behavior is observed if the magnetization of K is reversed relative to the ^3He magnetization. The system becomes dynamically unstable and spontaneously develops transverse magnetization as shown in Fig. 5. For this data the pumping light was blocked, the quarter-wave plate rotated by 90° , and the light unblocked. After the decay of the transient response the ^3He magnetization ends up parallel to the K magnetization. We find analytically that the magnetization is dynamically unstable for $M_z^e M_z^n < 0$ if

$$-\frac{\gamma_n \gamma_e \lambda^2 M_z^e M_z^n T_e}{1 + [\gamma_e (B_z + \lambda M_z^n) T_e]^2} - \frac{1}{T_{2n}} > 0. \quad (4)$$

The effect is much more pronounced near the compensation point, where $\gamma_e (B_z + \lambda M_z^n) T_e \ll 1$.

Finally we study the operation of the system as a self-compensated comagnetometer. To model CPT-violating

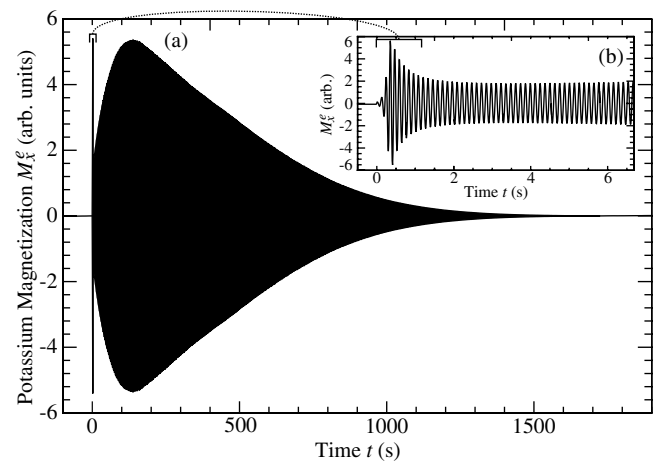


FIG. 5. (a) Spontaneous transverse oscillations following a reversal of K magnetization and (b) initial growth of the spontaneous oscillations. Note the similarity in the shape of the initial growth of spontaneous oscillations with the decay of the transient shown in Fig. 4.

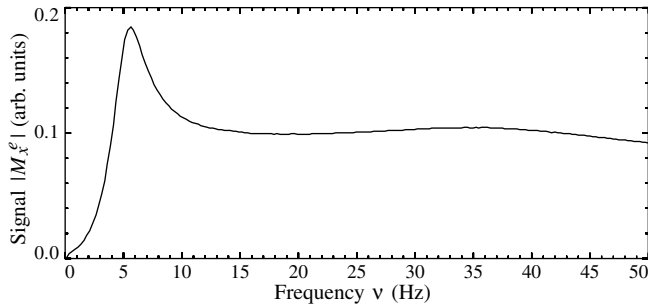


FIG. 6. The frequency response of the K- ^3He system at the compensation point to changes in the B_y field. As $\nu \rightarrow 0$ the ^3He adiabatically follows the external field \mathbf{B} while its magnetization cancels B_y , so that K does not see any changes in the magnetic field.

effects or other nonmagnetic interactions we include in the Bloch equations additional magneticlike fields b^e and b^n that couple only to the electron or nuclear spin. It can be shown that for slow changes of the magnetic field, the response of the magnetometer is given by

$$M_x^e = \frac{M_z^e[\lambda M_z^n b_y^n + (B_z + \lambda M_z^e)b_y^e]\gamma_e T_e/B_z}{1 + [(B_z + \lambda M_z^n + \lambda M_z^e)\gamma_e T_e]^2}. \quad (5)$$

The self-compensation condition is given by the equation $B_z + \lambda M_z^n + \lambda M_z^e = 0$. When B_z is tuned to this compensation point the magnetometer response simplifies to $M_x^e = M_z^e \gamma_e T_e (b_y^n - b_y^e)$ using the fact that $\lambda M_z^e \ll B_z$. Thus, at the compensation point the response to slow changes of normal magnetic field $B_y = b_y^n = b_y^e$ vanishes while the sensitivity to anomalous fields ($b_y^n \neq b_y^e$) remains. The frequency response of the comagnetometer to the B_y field at the compensation point is shown in Fig. 6. As expected, at low frequencies the response to B_y vanishes, while at higher frequencies there is a narrow peak corresponding to the ^3He resonance and a broader K response. Compensation factors greater than 100 have been achieved. The compensation point is found by applying a modulation to the B_y field and tuning the B_z field to minimize the response of the magnetometer. We have previously demonstrated that K-K spin-exchange broadening is suppressed for the K magnetometer operating at high density and small magnetic field, resulting in a relatively long value of T_e [18]. We demonstrated magnetic field sensitivity of $10 \text{ fT}/\sqrt{\text{Hz}}$, while shot-noise sensitivity can reach down to $2 \times 10^{-18} \text{ T}/\sqrt{\text{Hz}}$. The same magnetic field sensitivity is expected for the comagnetometer operation.

In conclusion, we have discussed coherent spin-exchange interactions of ^3He and K ensembles. We observed several novel effects, such as an ‘‘avoided level crossing’’ of spin precession frequencies and a dynamic

instability of the system with opposite magnetizations. We have also shown how the coupled system can be operated as a self-compensated comagnetometer. Such a comagnetometer can be used for tests of *CPT* and Lorentz symmetries, as well as searches for mass-spin coupling [21] and other precision measurements.

We would like to thank Will Happer for helpful discussions. This work was supported by NIST, NSF, and the Packard Foundation.

-
- [1] T.G. Walker and W. Happer, *Rev. Mod. Phys.* **69**, 629 (1997).
 - [2] M. A. Rosenberry and T. E. Chupp, *Phys. Rev. Lett.* **86**, 22 (2001).
 - [3] D. Bear, R. E. Stoner, R. L. Walsworth, V. A. Kostelecky, and C. D. Lane, *Phys. Rev. Lett.* **85**, 5038 (2000).
 - [4] M. S. Albert *et al.*, *Nature (London)* **370**, 199 (1994).
 - [5] S. R. Schaefer, G. D. Cates, T. R. Chien, D. Gonatas, W. Happer, and T. G. Walker, *Phys. Rev. A* **39**, 5613 (1989).
 - [6] N. R. Newbury *et al.*, *Phys. Rev. A* **48**, 558 (1993).
 - [7] A. S. Barton, N. R. Newbury, G. D. Cates, B. Driehuys, H. Middleton, and B. Saam, *Phys. Rev. A* **49**, 2766 (1994).
 - [8] M. V. Romalis and G. D. Cates, *Phys. Rev. A* **58**, 3004 (1998).
 - [9] R. E. Stoner and R. L. Walsworth, *Phys. Rev. A* **66**, 032704 (2002).
 - [10] P. L. Auer, H. Hurwitz, Jr., and R. D. Miller, *Phys. Fluids* **1**, 501 (1958).
 - [11] H. Hasegawa, *Prog. Theor. Phys.* **21**, 483 (1959).
 - [12] S. E. Barnes, *Adv. Phys.* **30**, 801 (1981).
 - [13] V. A. Kostelecky and C. D. Lane, *Phys. Rev. D* **60**, 116010 (1999).
 - [14] M. Romalis, J. Allred, and R. Lyman, in *CPT and Lorentz Symmetry II*, edited by V. A. Kostelecky (World Scientific, Singapore, 2002), p. 235.
 - [15] B. J. Venema, P. K. Majumder, S. K. Lamoreaux, B. R. Heckel, and E. N. Fortson, *Phys. Rev. Lett.* **68**, 135 (1992).
 - [16] Possible use of Rb and ^3He masers as a comagnetometer is discussed in R. E. Stoner, *CPT and Lorentz Symmetry*, edited by V. A. Kostelecky (World Scientific, Singapore, 1999), p. 201.
 - [17] A. B. Baranga *et al.*, *Phys. Rev. Lett.* **80**, 2801 (1998).
 - [18] J. C. Allred, R. N. Lyman, T. W. Kornack, and M. V. Romalis, *Phys. Rev. Lett.* **89**, 130801 (2002).
 - [19] G. D. Cates, S. R. Schaefer, and W. Happer, *Phys. Rev. A* **37**, 2877 (1988).
 - [20] V. A. Kartoshkin, *Opt. Spectrosk.* **79**, 26 (1995).
 - [21] A. N. Youdin, D. Krause, Jr., K. Jagannathan, L. R. Hunter, and S. K. Lamoreaux, *Phys. Rev. Lett.* **77**, 2170 (1996).